Int. J. Electrochem. Sci., 14 **(2019)** 4546 – 4556, doi: 10.20964/2019.05.35

International Journal of
ELECTROCHEMICAL
SCIENCE
www.electrochemsci.org

Electrochemical Characterization of Anodic Oxide Film on TC11 Alloy in Sulfate Solution at High Temperature and High Pressure

Lei Zha[1,2], *Heping Li*[1,*], *Ning Wang*[1]

[1] Key Laboratory of High-temperature and High-pressure Study of the Earth's Interior, Institute of Geochemistry, Chinese Academy of Sciences, Guiyang 550081, P. R. China
[2] University of Chinese Academy of Sciences, Beijing 100049, P. R. China
[*]E-mail: liheping@vip.gyig.ac.cn

Received: 8 January 2019 / *Accepted:* 26 February 2019 / *Published:* 10 April 2019

The oxide films studied in this work were prepared by potentiostatic anodic oxidation of TC11 alloy in 0.01 M sodium sulfate solutions at different anodizing potentials at 300 ℃ and 10 MPa. This work aimed to study the effect of film formation potential on the passivity of the TC11 alloy in high temperature sodium sulfate. Electrochemical impedance spectroscopy (EIS) combined with Mott-Schottky (MS) measurements were used to investigate the electrochemical properties of the as-grown anodic passive films on theTC11 alloy. The experimental data were also interpreted using the point defect model (PDM). An equivalent circuit was proposed to fit the EIS experimental data, leading to the determination of oxide film resistance, with the increase of the film-forming potential film resistance increase. According to the MS analysis, the anodic oxidation passivation film on the TC11 alloy was an n-type semiconductor, and the main point defects were oxygen vacancies. The calculated donor density was found to decrease exponentially with an increase in the film-forming potential, while the passive film thickness increases linearly with the applied potential. These experimental conclusions were consistent with the theoretical predictions of the PDM.

Keywords: TC11 alloy; Anodic oxide film; EIS; Mott-Schottky; High temperature

1. INTRODUCTION

Titanium and its alloys have excellent corrosion resistance due to the passivation film formed on their surfaces, which insulates the matrix from further contact with the corrosive medium [1]. However, as promising structural materials, during service they are exposed to harsh conditions, such as high temperature, high pressure, and corrosive ions [2, 3]. Aggressive corrosive media will cause a certain

degree of damage to the passive film, thus affecting the protective effect of the passive film on the matrix; as a result, the corrosion of titanium materials will still occur [4-6].

Anodic oxidation is the most commonly used method for improving the corrosion resistance of metals and alloys. It can effectively generate a stable and compact oxide film to protect the substrate against corrosion for a certain period of time. The properties of the anodic oxide film formed on the surface of titanium materials depend on electrolyte composition, temperature, initial surface state, pH value, applied potential, electrolysis time and other factors [7-11]. In industry, titanium and its alloys are often anodized in acid, salt or other solutions at tens of volts. Anodic oxidation of titanium is usually carried out at ambient temperature. The applied potential is a key factor affecting the properties and thickness of the film.

The electrical properties of the passive film formed by anodic oxidation on the surface of titanium materials are very important for understanding the corrosion resistance and corrosion mechanism of the film. Recently, there have been many studies on the electronic properties of the passive films of titanium and titanium alloys [12-20]. The passivation film is mainly composed of semiconductor titanium oxides, and its blocking effect on ions is closely related to the semiconductor properties of this oxide film. The n-type semiconductor behavior is observed, and the main electron donor species in the oxide layer on the titanium surface have been confirmed to be oxygen vacancies and/or cation interstitial defects [13, 16-18, 20]. The point defect model (PDM) predicted the microscopic mechanism of the growth/rupture in the passive film, which is based on the migration of point defects in the film under the influence of an internal electric field [21, 22]. Based on PDM, the concentration and diffusion properties of defects in passive films can be calculated. Therefore, PDM is often used for quantitative analysis of stabilized passivation films.

The TC11 alloy may be be promising for use as a structural material, and it is widely used as a lining material for autoclaves and as a valve material. During the service period, the TC11 alloy is exposed to harsh corrosive, high-temperature and high-pressure environments [5]. Despite the relatively extensive works published on titanium passive films, there seems to be a lack of study on the passive film formed on TC11 alloys in high-temperature and high-pressure environments. The objective of the present work is to characterize the passive film that forms on the TC11 alloy in 0.01 M Na_2SO_4 aqueous phase at 300 ℃ and 10 MPa. In this study, the oxide films were produced by potentiostatic anodic oxidation of the TC11 alloy in 0.01 M sodium sulfate solutions at 300 ℃ and 10 MPa at different anodizing potentials. The electrochemical behavior of the as prepared films was studied with EIS and MS measurements. Experimental data were also interpreted with the PDM.

2. EXPERIMENTAL

2.1. Material, solution and electrochemical cell

The material tested was a TC11 alloy (where the nominal composition (wt.%) is 6.5% Al, 3.5% Mo, 1.5% Zr, 0.3% Si, Bal. Ti). Titanium alloy electrodes were fabricated from 1 cm diameter rods of TC11. All samples were successively abraded to 1500 grit with SiC paper, cleaned with ethanol and

deionized water and air-dried prior to tests. The solution (0.01 M Na_2SO_4) was prepared from analytical grade sodium sulfate and deionized water. Argon was injected for 30 minutes to remove oxygen from the system. The experiments were conducted at a high temperature of 300 ℃, and the balanced pressure was approximately 10 MPa.

The electrochemical measurements were performed in a homemade multifunctional autoclave with three electrodes. The counter electrode was a homemade platinum electrode. An external pressure-balanced Ag/AgCl electrode filled with 0.1 M KCl solution was applied as the reference electrode. The reference electrode was maintained at room temperature (25 ℃) and system pressure via the Luggin capillary. The thermal diffusion potential generated by the temperature gradient can be calibrated according to the work of Macdonald [23], and the equation is as follows:

$$\Delta E_{\mathrm{SHE}} = \Delta E_{\mathrm{obs}} + 0.2866 - 0.001\Delta T + 1.745 \times 10^{-7}\Delta T^2 - 3.03 \times 10^{-9}\Delta T^3$$

where ΔE_{obs} is the observed potential of the working electrode vs. the Ag/AgCl reference electrode, and ΔE_{SHE} is the corresponding potential vs. the standard hydrogen electrode (SHE) at the experimental temperature. $\Delta T = T - 298.15$ K, where T is the experimental temperature. All potential values in the text are relative to the SHE if they are not specifically mentioned.

2.2. Electrochemical tests

All electrochemical measurements were performed using a Princeton applied research (PAR) 2263 electrochemical station. The potentiodynamic polarization experiments were performed from –0.3 V vs. OCP up to 1.6 V with a scan rate of 2 mV/s. Prior to the experiment, the samples were cathodically polarized at –1 V vs. the reference electrode (Ag/AgCl, [Cl^-]=0.1 M) for 30 minutes, which provided a reproducible initial surface state. Four potentials within the passive region were chosen for potentiostatic film growth. Films were grown at each selected potential for 1 h to ensure that the system was in steady-state. After each film growth period, electrochemical impedance spectroscopy (EIS) measurements were performed. The EIS tests were performed using a sinusoidal signal of 10 mV amplitude in the frequency range of 10 m-100 kHz with a sampling rate of 8 points per decade. The EIS plots were analyzed with Zsimpwin software. Mott-Schottky experiments were performed at 1 kHz during a negative potential scan from 1.0 V to 0 V.

3. RESULTS AND DISCUSSION

3.1. Polarization measurements

The potentiodynamic polarization curve of the TC11 alloy electrode in 0.01 M Na_2SO_4 at 300 ℃ and 10 MPa is shown in Fig. 1. It is observed that TC11 exhibits a stable passivation behavior from 0 V to 1.0 V in 0.01 M Na_2SO_4.

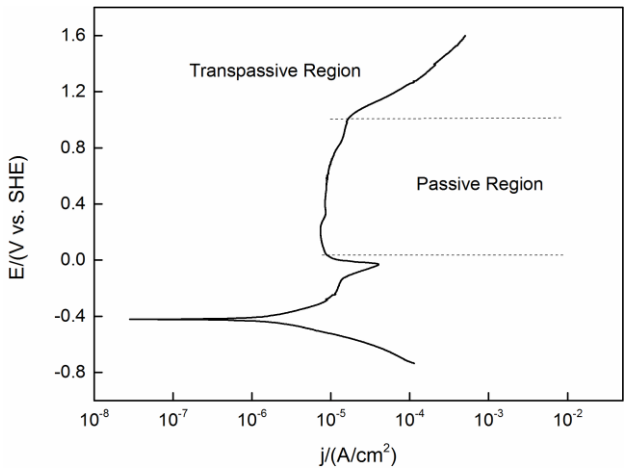

Figure 1. Polarization curve of TC11 alloy measured in 0.01 M Na_2SO_4 solution at 300 ℃ and 10 MPa. Scan in positive direction at 2 mV/s.

To study the properties of the oxide film produced by anodic oxidation, four different potentials (namely, 0.2, 0.4, 0.6, and 0.8 V) were selected in the passivation region to generate a passive layer on the electrode surface. In the anodic oxidation process, the variation in the current density over time was also recorded, as shown in Fig. 2. The current density decreases rapidly at the beginning and then gradually stabilizes. The exponential decay of the current density with time is attributed to the formation and growth of the passivation film on the alloy electrode surface.

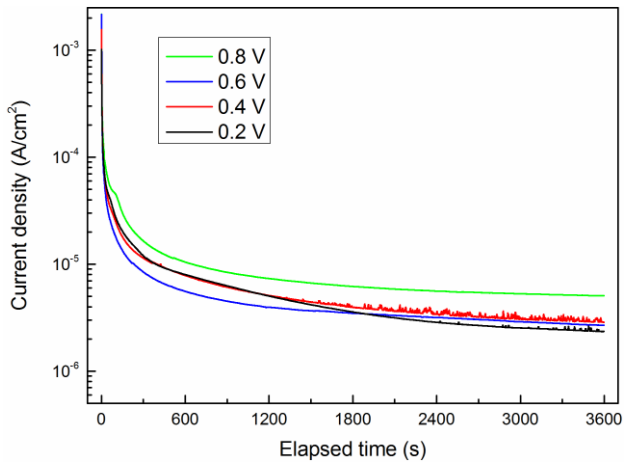

Figure 2. Evolution of the current density measured during the application of different passive potentials.

The relationship between the steady-state passivation current density (j_{ss}) values and the film formation potentials is shown in Fig. 3. It seems that there is no obvious relationship between the steady-state current and the film formation potential. The average steady-state passive current density is approximately 3.2 μA/cm^2.

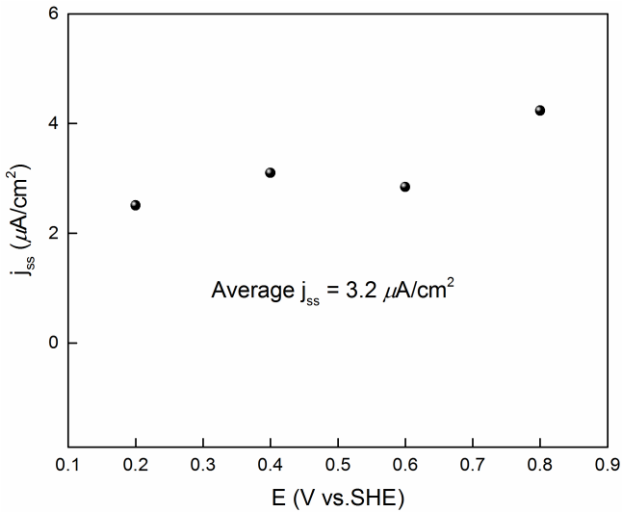

Figure 3. Steady-state passive current density obtained during the potentiostatic growth of the passive films at different film formation potentials.

3.2. EIS measurements

The impedance spectrum tests were conducted after the oxide films were formed. The results from the EIS measurements performed on the anodic oxidation passive films, including the Nyquist plots and Bode diagrams, are shown in Fig. 4. All impedance spectra exhibited similar shapes and identical features over the frequency range tested. It shows that the oxide films formed at different potentials have a similar growth mechanism.

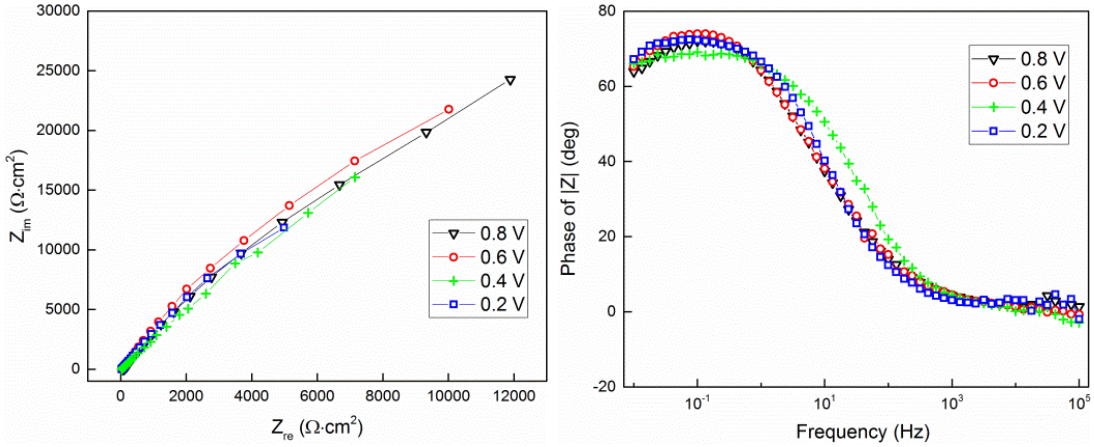

Figure 4. Impedance spectra for TC11 alloy in 0.01 M Na_2SO_4 as a function of formation potential: Nyquist plots and Bode plots.

The measured impedance spectra are fitted with the equivalent electronic circuit, $R_s(R_1Q_1)(R_2Q_2)$. In this equivalent circuit, R_s is the solution resistance, Q_1 is the constant phase element (CPE) for the double-layer, R_1 is the charge transfer resistance, Q_2 is the CPE for the passive film and R_2 is the passive film resistance. The fitting results are shown in Table 1. It can be found that with the increase in the film-forming potential, the film resistance increases, while the film capacitance decreases. This means

that as the film-forming potential increases, the passive film becomes more compact and uniform, and the protective effect of the film on the matrix is enhanced. The results of the EIS analysis are consistent with the MS analysis results here in after.

Table 1. Calculated film resistance and film capacitance from the impedance diagrams of TC11 alloy in 0.01 M Na_2SO_4 solution.

E (V)	R_{film} (kΩ·cm^2)	C_{film} (F/cm^2)
0.2	18.80	0.003257
0.4	22.60	0.002075
0.6	26.22	0.001568
0.8	28.29	0.001424

3.3. Mott-Schottky analysis

Mott-Schottky analysis is often used to determine the type of semiconductor conductivity of the oxide film and to obtain the density of the dopant within the oxide film. The following formulas are used to determine whether semiconductors are n-type or p-type, respectively [24]:

$$\frac{1}{C_{SC}^2} = \frac{2}{\varepsilon\varepsilon_0 e N_D}\left(E - E_{FB} - \frac{k_B T}{q}\right) \text{ for n-type semiconductors} \quad (1)$$

$$\frac{1}{C_{SC}^2} = -\frac{2}{\varepsilon\varepsilon_0 e N_A}\left(E - E_{FB} - \frac{k_B T}{q}\right) \text{ for p-type semiconductors} \quad (2)$$

where C_{SC} is the space charge capacitance, e represents the elementary charge, N refers to the carrier concentration for the acceptor and donor (cm^{-3}), ε is the dielectric constant of the passive film (=55 [25]), ε_0 is the vacuum dielectric constant (8.854×10^{-14} F/cm), k_B is the Boltzmann constant (1.38×10^{-23} J/K), T is the absolute temperature and E_{FB} is the flat band potential. The interfacial capacitance, C, is obtained from Sikora and Macdonald [26]:

$$C = -\frac{1}{\omega Z_{img}} \quad (3)$$

where Z_{img} is the imaginary component of the impedance and ω is the angular frequency. The measured capacitance can be regarded as the C_{SC}, if the double layer capacitance is negligible [27, 28].

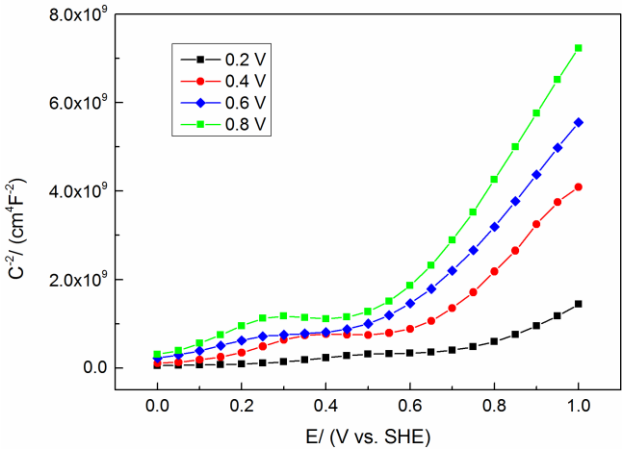

Figure 5. Mott-Schottky plots of C^{-2} as a function of potential for the passive film on TC11 alloy formed at the potentials of 0.2, 0.4, 0.6 and 0.8 V in 0.01 M Na_2SO_4 at 300 ℃ and 10 MPa.

Fig. 5 shows the Mott-Schottky plots of the passive film formed on the surface of the TC11 alloy electrode at different film-forming potentials in sodium sulfate solution. It can be seen from the figure that all four lines have a positive slope, indicating that the generated passivating film exhibits the characteristics of an n-type semiconductor. According to formula (1), the donor density (N_D) of the passive film formed at different potentials can be calculated from the slope of the linear section of the curve. As the film formation potential increases, the slope of the linear part increases gradually, indicating that the donor density in the passivating film decreases with increasing film formation potential, which coincides with the prediction of the PDM [29]. Note that the MS graph shows a relatively small linear region (0.6 V-1.0 V). It is believed that the donor type and/or donor density vary with the potential, resulting in the appearance of the nonlinear region [30]. Nevertheless, Sikora [29] and Goossens [31] believed that this kind of nonlinear behavior was due to the passive film thickness increasing linearly with the applied potential.

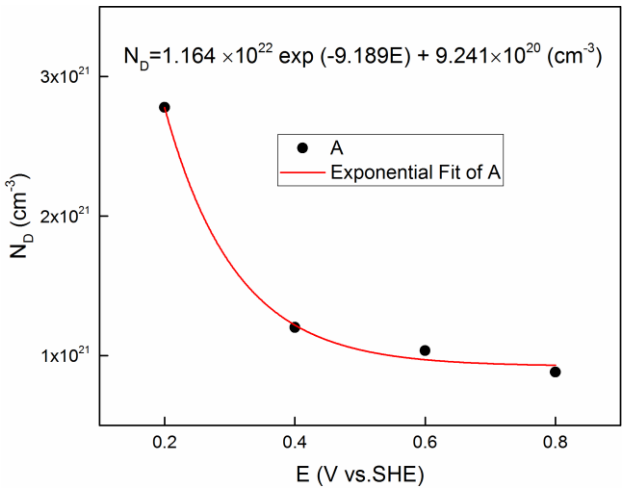

Figure 6. Donor densities of the passive film formed on the TC11 alloy in 0.01 M Na_2SO_4 as a function of film formation potential. (The dots are experimental data and the solid line is the fitting curve)

Generally, the main forms of defects in an n-type semiconductor film are oxygen vacancies and/or cation interstitials. Thus, the two possible dopants in this case are titanium interstitials and oxygen vacancies. By examining the atomic radius of oxygen and titanium, it can be found that the atomic radius of titanium is significantly larger than that of oxygen. As a result, the energy required for the transition of titanium interstitials in the film is greater than that of oxygen vacancies. Therefore, the main form of defects present in the passivation film on the TC11 alloy should be oxygen vacancies. This excludes a change in donor-type as being the reason for the nonlinearity mentioned above.

Fig. 6 shows the relationship curve between donor density and film-forming potential. The fitting results in Fig. 6 show that the donor density decreases exponentially as the film-forming potential increases. Sikora and Macdonald have reported donor density values similar to this work and have also observed a decrease in donor density with increasing film formation potential [29, 32]. The internal structure of the passivated film is more uniform at a higher potential, and fewer impurities are contained in the film, thereby reducing the density of impurities in the film. On the other hand, according to thermodynamic theory, as the passivation potential increases, the valence state of titanium ions will increase, correspondingly. The increase of high-valence metal ions leads to a decrease in the concentration of free electrons in the semiconductor film; that is, the donor concentration decreases, and the formation of the film tends to be more complete. In addition, according to the work of Sikora [29], the increase in the film-forming potential can inhibit an increase in the concentration of oxygen vacancies in the passive film to some extent.

Based on the PDM theory [29], the relationship between donor density (N_D) and the film formation potential (E) is as follows:

$$N_D = \omega_1 \, exp(bE) + \omega_2 \quad (4)$$

where ω_1, ω_2 and b are constants. It can be inferred from formula (4) that the donor density (N_D) decreases exponentially with an increase in the film formation potential; the experimental results are consistent with the theoretical analysis of PDM [29]. The exponential relationship between N_D and the film formation potential can be obtained by nonlinear fitting the data with relevant software, as shown in Fig. 6:

$$N_D = 1.164 \times 10^{22} exp(-9.189E) + 9.241 \times 10^{20} \ (cm^{-3}) \quad (5)$$

The diffusion coefficient can be derived from formula (6) as follows [29, 33]:

$$D_0 = -\frac{J_0}{2K\omega_2} = -\frac{J_0 RT}{2F\omega_2 k} \quad (6)$$

$$J_0 = -\frac{j_{ss}}{2e} \quad (7)$$

where $K = \frac{kF}{RT}$, k represents the electric field strength in the passive film, and j_{ss} is obtained from Fig. 3. According to previous work [34], the k value for the oxide film on the titanium surface is 2.6×10^6

V/cm. Therefore, it can be assumed that the *k* value of the passive film formed on the TC11 alloy in 0.01 M sodium sulfate is approximately 10^6 V/cm. Substituting the relevant parameters j_{ss} (3.2×10^{-6} A/cm^{-2}), *e* (1.602×10^{-19} C), *k* (10^6 V/cm), ω_2 (9.241×10^{20} cm^{-3}), *R* (8.314 J/mol K), *T* (573 K) and *F* (96500 C/mol) into Eqs. (6) and (7) yields $D_0=2.667\times10^{-16}$ cm^2/s. Considering the error caused by the valuation *k*, the point defect diffusion coefficient of the TC11 passivation film in 0.01 M sodium sulfate is estimated to be in the range of 10^{-17}-10^{-16} cm^2/s.

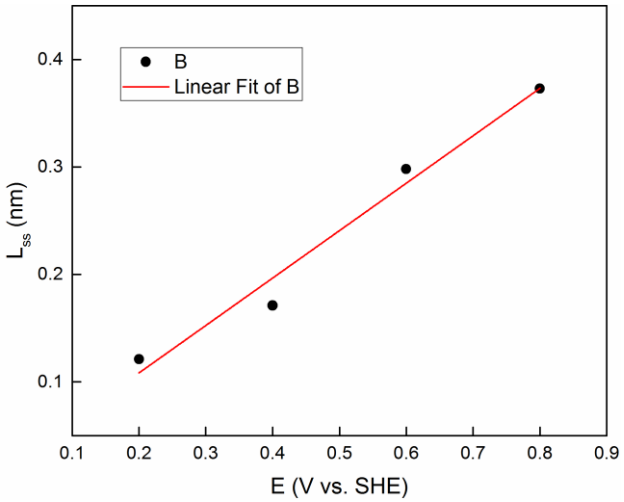

Figure 7. Film thickness as a function of the formation potential. Thickness was measured after each 1 h film growth.

Fig. 7 shows the linear relationship between the thickness of the film under steady-state conditions (L_{ss}) and the film-forming potential. Macdonald also reported a similar linear relationship between L_{ss} and the film-forming potential [35-37]. The steady-state film thickness was calculated by the following formula [29, 32]:

$$L_{ss} = \frac{\varepsilon\varepsilon_0}{C} \quad (8)$$

where *C* is the capacitance measured after 1 h of constant potential polarization at a frequency of 1000 Hz, which is a commonly used frequency for this type of analysis. It is assumed that the EIS is essentially capacitive at this frequency, and which the measured capacitance is almost frequency independent. The calculated thickness ranges from approximately 0.605 nm at 0.2 V to 1.865 nm at 0.8 V. The linear variation in the film thickness with the film-forming potential indicates that the spatial electric field intensity within the film is independent of film formation potential. This indicates that the film-forming potential is not sensitive to the electric field intensity of the barrier layer, which is the basis of the PDM. In addition, the driving force of defect transmission on the barrier layer is independent of the applied potential.

Furthermore, the uniform corrosion rate can be calculated by using the steady-state passivation current density based on the PDM using the following formula [37]:

$$\frac{\mathrm{d}L}{\mathrm{d}t} = \frac{\overline{M}}{\bar{z}F\rho} i_{\mathrm{ss}} \quad (9)$$

where $\overline{M}$ is the composition-averaged atomic weight, $\bar{z}$ is the oxidation number, and ρ is the density of the titanium alloy (4.50 g/cm^3). The corrosion rate calculated from Eq. (9) is 8.89×10^{-11} cm/s or 28.035 μm/year. This corresponds to approximately 2.8 mm of corrosion penetration in one hundred years of service.

Our previous studies showed that the TC11 alloy was subject to a certain degree of electrochemical corrosion in a high-temperature and high-pressure sodium sulfate aqueous solution [5]. The passive current density is approximately 27 μA/cm^2 under the same experimental conditions (0.01 M Na_2SO_4, 10 MPa 300 ℃). However, after anodic oxidation, the steady-state passive current density decreases significantly, that is approximately 3.2 μA/cm^2 as presented in this paper. The corrosion resistance of the TC11 alloy was significantly improved by low potential anodic oxidation.

4. CONCLUSIONS

The results of potentiodynamic polarization show that TC11 displays an obvious stable passivation range (0 to 1 V vs. SHE) in 0.01 M Na_2SO_4 solution at 300 ℃ and 10 MPa. Potentiostatic polarization reveals that there is no obvious relationship between the passive current density of the TC11 alloy and the film-formation potential. According to the Mott-Schottky analysis, the anodic oxidation passivation films on the TC11 alloy is an n-type semiconductor, and the main point defects are oxygen vacancies. The calculated donor density is found to decrease exponentially with an increase in the film forming-potential, while the passive film thickness increases linearly with the applied potential. These experimental conclusions are consistent with the theoretical predictions of the point defect model. The point defect diffusion coefficient of the TC11 passivation film in 0.01 M sodium sulfate is estimated to be in the range of 10^{-17}-10^{-16} cm^2/s. The corrosion resistance of the TC11 alloy was significantly improved by low potential anodic oxidation.

ACKNOWLEDGEMENTS
This research was financially supported by the National Key R&D Program of China (Grant NO. 2016YFC0600104) and the ‘‘135” Program of the Institute of Geochemistry, Chinese Academy of Sciences (CAS).

References

1. R. M. Fernandez-Domene, E. Blasco-Tamarit, D. M. Garcia-Garcia and J. G. Anton, *J. Electrochem. Soc.*, 161 (2014) C25.
2. J. Vaughan, P. Reid and A. Alfantazi, *Hydrometallurgy*, 101 (2010) 156.
3. J. S. Grauman and T. Say, *Adv. Mater. Process.*, 157 (2000) 25.
4. J. Liu, A. Alfantazi and E. Asselin, *J. Electrochem. Soc.*, 162 (2015) C189.
5. L. Zha, H. P. Li, N. Wang, S. Lin and L. P. Xu, *Int. J. Electrochem. Sci.*, 12 (2017) 5704.
6. S. B. Basame and H. S. White, *J. Electrochem. Soc.*, 147 (2015) 1376.

7. C. E. B. Marino and L. H. Mascaro, *Int. J. Electrochem.*, 2011 (2011) 7.
8. C. E. B. Marino, P. A. P. Nascente, S. R. Biaggio, R. C. Rocha-Filho and N. Bocchi, *Thin Solid Films*, 468 (2004) 109.
9. Y.-T. Sul, C. B. Johansson, Y. Jeong and T. Albrektsson, *Med. Eng. Phys.*, 23 (2001) 329.
10. A. A. Mazhar, *J. Appl. Electrochem.*, 20 (1990) 494.
11. M. E. Sibert, *J. Electrochem. Soc.*, 110 (1963) 65.
12. J. R. Birch and T. D. Burleigh, *Corrosion*, 56 (2000) 1233.
13. A. M. Schmidt, D. S. Azambuja and E. M. A. Martini, *Corros. Sci.*, 48 (2006) 2901.
14. E. N. Paleolog, A. Z. Fedotova, O. G. Derjagina and N. D. Tomashov, *J. Electrochem. Soc.*, 125 (1978) 1410.
15. M. C. K. Sellers and E. G. Seebauer, *Thin Solid Films*, 519 (2011) 2103.
16. Z. L. Jiang, X. Dai and H. Middleton, *Mater. Chem. Phys.*, 126 (2011) 859.
17. D. S. Kong, W. H. Lu, Y. Y. Feng, Z. Y. Yu, J. X. Wu, W. J. Fan and H. Y. Liu, *J. Electrochem. Soc.*, 156 (2009) C39.
18. B. Roh and D. D. Macdonald, *Russ. J. Electrochem.*, 43 (2007) 125.
19. D. G. Li, J. D. Wang and D. R. Chen, *Electrochim. Acta*, 60 (2012) 134.
20. D. Sazou, K. Saltidou and M. Pagitsas, *Electrochim. Acta*, 76 (2012) 48.
21. D. D. Macdonald, *J. Electrochem. Soc.*, 139 (1992) 3434.
22. D. D. Macdonald, *Russ. J. Electrochem.*, 48 (2012) 235.
23. D. D. Macdonald, A. C. Scott and P. Wentrcek, *J. Electrochem. Soc.* 126 (1979) 908.
24. A. D. Paola, *Electrochim. Acta*, 34 (1989) 203.
25. C. S. Enache, J. Schoonman and R. V. Krol, *J. Electroceram.*, 13 (2004) 177.
26. E. Sikora and D. D. Macdonald, *Electrochim. Acta*, 48 (2002) 69.
27. R. S. Morrison, *Electrochemistry at Semiconductor and Oxidised Metal Electrodes*, Springer US, (1980) Plenum, New York.
28. F. Gaben, B. Vuillemin and R. Oltra, *J. Electrochem. Soc.*, 151 (2004) B595.
29. E. Sikora, J. Sikora and D. D. Macdonald, *Electrochim. Acta*, 41 (1996) 783.
30. M. Bojinov, G. Fabricius, T. Laitinen, K. Mäkelä, T. Saario and G. Sundholm, *Electrochim. Acta*, 45 (2000) 2029.
31. A. Goossens, M. Vazquez and D. D. Macdonald, *Electrochim. Acta*, 41 (1996) 35.
32. E. Sikora and D. D. Macdonald, *Solid State Ionics*, 94 (1997) 141.
33. S. J. Ahn and H. S. Kwon, *Electrochim. Acta*, 49 (2004) 3347.
34. D. Ellerbrock and D. D. Macdonald, *J. Solid State Electrochem*, 18 (2014) 1485.
35. D. D. Macdonald and A. Sun, *Electrochim. Acta*, 51 (2006) 1767.
36. D. D. Macdonald, *J. Nucl. Mater.*, 379 (2008) 24.
37. I. Nicic and D. D. Macdonald, *J. Nucl. Mater.*, 379 (2008) 54.